

---

# Gaussian DAGs on Network Data

---

**Hangjian Li**

Department of Statistics  
University of California, Los Angeles  
Los Angeles, CA 90095  
lihangjian123@ucla.edu

**Qing Zhou**

Department of Statistics  
University of California, Los Angeles  
Los Angeles, CA 90095  
zhou@stat.ucla.edu

## Abstract

The traditional directed acyclic graph (DAG) model assumes data are generated independently from the underlying joint distribution defined by the DAG. In many applications, however, individuals are linked via a network and thus the independence assumption does not hold. We propose a novel Gaussian DAG model for network data, where the dependence among individual data points (row covariance) is modeled by an undirected graph. Under this model, we develop a maximum penalized likelihood method to estimate the DAG structure and the row correlation matrix. The algorithm iterates between a decoupled lasso regression step and a graphical lasso step. We show with extensive simulated and real network data, that our algorithm improves the accuracy of DAG structure learning by leveraging the information from the estimated row correlations. Moreover, we demonstrate that the performance of existing DAG learning methods can be substantially improved via de-correlation of network data with the estimated row correlation matrix from our algorithm.

## 1 Introduction

### 1.1 Background

Directed acyclic graphs (DAGs) or Bayesian networks (BNs) are widely used to represent conditional independence and causal relations among random variables. Graphical models based on DAGs have a variety of applications, including genetics [15], causal inference [20], machine learning [18], etc. Therefore, in the past decades, extensive research has been done to recover the structure of DAGs from observational and experimental data. Most structure learning algorithms for DAGs can be categorized as either score-based or constraint-based. Score-based methods search for the optimal DAG by maximizing a scoring function (e.g., MDL [22], BIC [7], Bayesian scores [14, 5]) with various search strategies, such as order-based search [23, 24, 31], greedy search [21, 4], and coordinate descent [9, 3, 11]. Constraint-based methods [26, 32] perform conditional independence tests among variables to construct a skeleton and then orient some of the edges. There are also hybrid methods [12] that combine the above two approaches.

The classical DAG learning problem is formulated as follows: Let  $X = (X_1, \dots, X_p) \in \mathbb{R}^{n \times p}$  be the data matrix consisting of  $n$  i.i.d observations  $x_i \in \mathbb{R}^p, i \in [n]$ , where  $x_i$  are generated from an underlying distribution  $\mathbb{P}$  defined by a DAG  $G^*$  on  $p$  nodes. The goal is to learn the structure of  $G^*$  from  $X$ . In this paper, we focus on the Gaussian DAG model which is equivalent to the following Gaussian linear structural equations model (SEM):

$$x_i = B^\top x_i + e_i, \quad e_i \sim \mathcal{N}_p(0, \Omega), \quad i \in [n], \quad (1)$$

where  $B = (\beta_{kj})_{p \times p}$  is the weighted adjacency matrix of  $G^*$  with edge set  $E = \{(k, j) : \beta_{kj} \neq 0\}$ , and  $\Omega = \text{diag}(\omega_1^2, \dots, \omega_p^2)$ . Given i.i.d. samples  $\{x_i\}_{i=1}^n$ , the goal is to estimate  $B$ , from which we will immediately get an estimated structure of  $G^*$ .

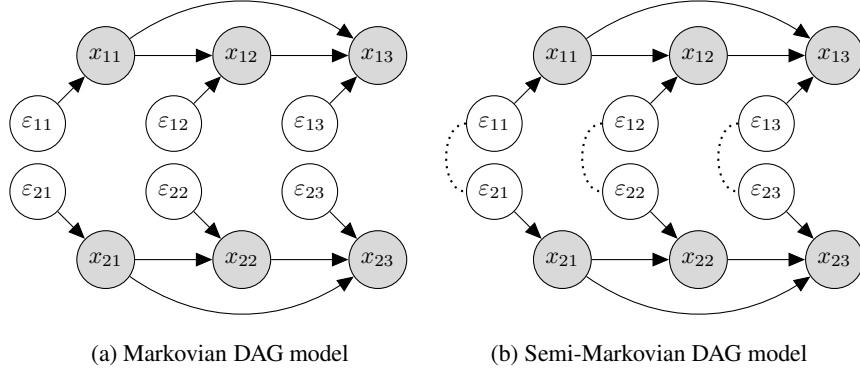


Figure 1: Graphical representations of the models in (1) and (2).

## 1.2 A model for network data

Independence among observed samples  $\{x_i\}_{i=1}^n$  is one of the main assumptions for all the aforementioned DAG learning methods. In real applications, however, it is highly likely to find dependence among the observations  $x_1, \dots, x_n$ . For example, when using a DAG to model the characteristics of an individual in a social network, the observed characteristics from different individuals may no longer be independent, since these individuals may belong to the same social group such as friends, family and colleagues, often sharing similar features. Another example is to model a gene regulatory network from individuals that are potentially linked genetically. This motivates our development of a novel Gaussian DAG model for network data.

A common way to model the dependence among observations is using an undirected graph  $\mathcal{G}$  with each node representing an observation  $x_i$  and each edge representing the conditional dependence between two observations given the rest. More explicitly, let  $A(\mathcal{G})$  be the adjacency matrix of  $\mathcal{G}$  so

$$x_i \perp\!\!\!\perp x_j | x_{\setminus\{i,j\}} \iff A(\mathcal{G})_{ij} = 0.$$

Suppose we observe not only the dependent samples  $\{x_i\}_{i=1}^n$  but also the matrix  $A(\mathcal{G})$ , i.e. the network structure among them. Recall  $X_j = (x_{1j}, \dots, x_{nj}) \in \mathbb{R}^n$  is the  $j$ th column in  $X$  and  $B = (\beta_{kj})_{p \times p}$  is the weighted adjacency matrix of the DAG  $G^*$ . We generalize the SEM (1) to

$$X_j = \sum_{k \in \Pi_j} \beta_{kj} X_k + \varepsilon_j, \quad \varepsilon_j = (\varepsilon_{1j}, \dots, \varepsilon_{nj}) \sim \mathcal{N}_n(0, \omega_j^2 \Sigma), \quad (2)$$

where  $\Sigma$  is positive definite with  $\text{diag}(\Sigma) = 1$ ,  $\Pi_j$  is the parent set of  $X_j$ , and  $\varepsilon_j$ 's are independent of each other. The constraint  $\text{diag}(\Sigma) = 1$  ensures the identifiability of  $\omega_j^2$  and  $\Sigma$ . Moreover, the support of the precision matrix  $\Theta = \Sigma^{-1}$  is restricted by  $\text{supp}(\Theta) \subseteq A(\mathcal{G})$ . Note that when  $\Sigma = I_n$ , the SEM (2) reduces to (1). Hence, the classical Gaussian DAG (1) is a special case of (2).

The distinction between (1) and (2) becomes more clear when we regard (2) as a semi-Markovian causal model [27]. Following its causal reading [20], we can represent each variable  $z_i$  in a DAG  $G$  on vertices  $\{z_1, \dots, z_p\}$  using a deterministic function:

$$z_i = f_i(\Pi_i, u_i), \quad i \in [p], \quad (3)$$

where  $\Pi_i$  is the parents of node  $z_i$  in  $G$  and  $u_i$  are noises, sometimes also referred to as background variables. The model (3) is *Markovian* if the noise variables  $u_i$  are jointly independent, and it is *semi-Markovian* if they are dependent. Now for a data matrix  $X$  with  $n = 2$  and  $p = 3$ , consider the DAG models implied, respectively, by (1) and (2) over all six random variables  $x_{11}, x_{12}, x_{13}, x_{21}, x_{22}, x_{23}$ . Under SEM (1) we model  $x_1 = (x_{11}, x_{12}, x_{13})$  and  $x_2 = (x_{21}, x_{22}, x_{23})$  using the same SEM and assume they are independent, as shown in Figure 1a.<sup>1</sup> In contrast, the model proposed in (2) allows observations to be dependent by relaxing the independence assumption between  $\varepsilon_{1k}$  and  $\varepsilon_{2k}$ ,  $k = 1, 2, 3$ . If we use dashed lines to link correlated background variables, we arrive at a

<sup>1</sup>Independent background variables are often omitted in the graph, but we include them here to better illustrate the differences between the two models.

semi-Markovian DAG model as shown in Figure 1b. For learning with such data, as in our case, the correlations among  $\varepsilon_i$  will reduce the effective sample size; therefore, we will have to take the distribution of the correlated  $\varepsilon_i$  into account. As demonstrated in our numerical experiments, naive application of existing methods that ignore the correlation among  $x_i$ 's often results in a large number of false positive edges.

**Contributions** This paper devises a new method for structure learning of DAGs from network data. By utilizing the correlation information from data, we are able to improve the accuracy of DAG estimation. Our specific contributions include the following: (i) When the nodes of the DAG are in natural ordering, we develop a maximum penalized likelihood algorithm based on block coordinate descent (BCD) to jointly estimate the DAG structure and the sample correlations. (ii) When the node ordering is unknown, we show empirically that our algorithm can still estimate the sample correlation accurately, which can be used to improve existing DAG learning methods via data de-correlation. We also prove the desired score-equivalence property for our proposed model.

In this paper, we restrict our attention mostly to undirected networks with a block-diagonal adjacency matrix for row correlations, which implies  $\Theta$  is block-diagonal. This type of network is widely seen in applications where individuals in a network form clusters: nodes in the same cluster are densely connected, whereas those from different clusters tend to have loose connections. More general network structures are considered in the numerical experiments in Section 3.2.

## 2 Estimation and algorithm

### 2.1 Regularized log-likelihood

Let  $\beta_j = (\beta_{1j}, \dots, \beta_{pj})$ . We reparameterize  $(B, \Omega)$  following [3] by defining  $\rho_j = 1/\omega_j$ ,  $\phi_{ij} = \beta_{ij}/\omega_j$ . Put  $\Phi = (\phi_{ij})_{p \times p}$  and  $D = \text{diag}(\rho_1^2, \dots, \rho_p^2)$ . Define an  $n \times n$  matrix:

$$S(\Phi, D) = \frac{1}{p} \sum_{j=1}^p (\rho_j X_j - X \phi_j) (\rho_j X_j - X \phi_j)^\top = \frac{1}{p} \sum_{j=1}^p \frac{1}{\omega_j^2} (X_j - X \beta_j) (X_j - X \beta_j)^\top. \quad (4)$$

Under this reparametrization, the negative log-likelihood of  $X$  from (2) is

$$L(\Phi, D, \Theta | X) = -n \log \det D - p \log \det \Theta + \text{tr}(\Theta S(D, \Phi)). \quad (5)$$

In many applications, it is reasonable to assume that the underlying DAG is sparse. Therefore, we propose to minimize the  $\ell_1$ -penalized negative log-likelihood to jointly estimate a sparse DAG and  $\Theta$ :

$$\begin{aligned} \min_{\Phi, D, \Theta} \quad & L(\Phi, D, \Theta | X) + \lambda_1 \|\Phi\|_1 + \lambda_2 \|\Theta\|_1 \\ \text{subject to} \quad & \text{supp}(\Theta) \subseteq A, \text{diag}(\Theta^{-1}) = 1, \end{aligned} \quad (6)$$

where  $\|\Phi\|_1 = \sum_{j=1}^p \|\phi_j\|_1$ ,  $\|\Theta\|_1 = \sum_{i \neq j} |\theta_{ij}|$ , and  $A$  is the adjacency matrix of the network among individuals. The reparametrization above has two benefits: first, as explained in Section 2.2, it ensures the objective function in (8) is jointly convex with respect to  $(\rho_j, \phi_j)$ ; second, by imposing  $\ell_1$  penalty on  $\beta_{ij}/\omega_j$  instead of  $\beta_j$ , we also penalize the coefficients that overfit the data with very small  $\hat{\omega}_j$ .

**Remark 1.** Under the assumption of block-diagonal  $\Theta$ , the penalty term  $\|\Theta\|_1$  can be ignored when the block sizes are smaller than  $p$ . In this case, we simply set  $\lambda_2$  to be a small positive number.

Our model (2) defines a matrix normal distribution for  $X$ . This is due to the fact that  $\varepsilon = (\varepsilon_{ij})_{n \times p}$  in (2) follows a matrix normal distribution:

$$\varepsilon \sim \mathcal{N}_{n,p}(0, \Sigma, \Omega) \Leftrightarrow \text{vec}(\varepsilon) \sim \mathcal{N}_{np}(0, \Omega \otimes \Sigma),$$

where  $\text{vec}(\cdot)$  is the vectorization operator and  $\otimes$  is the Kronecker product. Then, the random matrix

$$X \sim \mathcal{N}_{n,p}(0, \Sigma, \Psi), \quad (7)$$

where  $\Psi = (I - B)^{-\top} \Omega (I - B)^{-1}$ . From the property of a matrix normal distribution, we can easily prove the following lemma which will come in handy when estimating row correlations  $\Sigma$  from different ordering of nodes. Given a permutation  $\pi$  of the set  $[p]$ , define  $P_\pi$  as the permutation matrix such that  $h P_\pi = (h_{\pi^{-1}(1)}, \dots, h_{\pi^{-1}(p)})$  for any row vector  $h = (h_1, \dots, h_p)$ .

**Lemma 1.** If  $X$  follows the model (2), then for any permutation  $\pi$  of  $[p]$  we have

$$XP_\pi \sim \mathcal{N}_{n,p}(0, \Sigma, P_\pi^\top \Psi P_\pi).$$

There are methods developed for estimating the two covariance matrices in (7). Previous studies usually assume we have  $N$  copies of  $X$  and the MLE exists when  $N \geq \max\{p/n, n/p\} + 1$  [6]. Allen and Tibshirani [2] proposed to use  $\ell_1$  penalization to estimate the covariance matrices when  $N = 1$ . More recent developments include the work on Kronecker graphical lasso [29, 33]. Our learning problem (2) is obviously different from these methods. We are not interested in estimating  $\Psi$  but a sparse factorization of  $\Psi$  represented by the DAG  $B$  or  $\Phi$ . Even for the row covariance  $\Sigma$ , we find that our formulation leads to much faster and accurate estimates, probably owing to the challenges in estimating  $\Psi$  when  $p \gg n$ .

## 2.2 Block coordinate descent

Inspired by the iterative algorithms in [3, 9] for penalized estimation of Gaussian DAGs, we develop a block coordinate descent (BCD) algorithm to solve (6) by alternating between optimizing over  $\Phi$ ,  $D$ , and  $\Theta$ . We first assume that a natural ordering among the nodes is given and will discuss the general unsorted DAGs later. Suppose the nodes are sorted according to the natural ordering. Let  $L$  be the lower triangular Cholesky factor of  $\Theta$  so that  $\Theta = L^\top L$ . When  $\Theta$ , and thus  $L$ , is fixed, we solve the following convex optimization problem for  $j = 1, \dots, p$ :

$$\min_{\rho_j, \phi_j} -n \log \rho_j^2 + \|\rho_j LX_j - LX \phi_j\|_2^2 + \lambda_1 \|\phi_j\|_1. \quad (8)$$

For each  $j$ , we optimize over  $\rho_j$  and  $\phi_j$  iteratively: given current value of  $\hat{\rho}_j$ , solving for  $\hat{\phi}_j$  becomes the standard Lasso problem. After obtaining the Lasso estimates  $\hat{\phi}_j$ , the estimate  $\hat{\rho}_j$  can be computed in closed-form:

$$\hat{\rho}_j = \frac{a_j^\top b_j + \{(a_j^\top b_j)^2 + 2n\|a_j\|_2^2\}^{1/2}}{2\|a_j\|_2^2}, \quad (9)$$

where  $a_j = LX_j \in \mathbb{R}^n$  and  $b_j = LX \phi_j \in \mathbb{R}^n$ . When we fix  $(\rho_j, \phi_j)$  to their current values, estimating  $\Theta$  becomes a modified graphical Lasso problem [8]:

$$\begin{aligned} \min_{\Theta} & -p \log \det(\Theta) + p \operatorname{tr}(S\Theta) + \lambda_2 \|\Theta\|_1 \\ \text{subj.} & \operatorname{supp}(\Theta) \subseteq A, \operatorname{diag}(\Theta^{-1}) = 1 \end{aligned} \quad (10)$$

where  $S$  is calculated as in (4).

Without the constraint  $\operatorname{diag}(\Theta^{-1}) = 1$ , (10) can be solved by standard solvers `glasso` [8] in R. But in general it is difficult to enforce this diagonal constraint during the optimization. Therefore, we come up with a two-step solution: We first optimize over  $\Theta$  without the diagonal restriction to obtain  $\hat{\Theta}_{\text{temp}}$ , and then normalize the resulting  $\hat{\Sigma}_{\text{temp}} = \hat{\Theta}_{\text{temp}}^{-1}$  into a correlation matrix  $\hat{\Sigma}$ . This relaxation to the original problem allows us to search for a minimizer in the space of positive definite matrices and then project the minimizer to the subset of correlation matrices. As a side effect of this relaxation-projection solution, the BCD algorithm no longer decreases the value of the objective function (6) monotonically. In order to guarantee monotonicity at each iteration, we adopt a heuristic line search method: After normalizing the graphical Lasso estimate  $\hat{\Theta}^{(t)}$ , we do an extra search between the latest two estimates  $\hat{\Theta}^{(t-1)}$  and  $\hat{\Theta}^{(t)}$  to find a minimum. Details of the algorithm can be found in Algorithm 1 below.

When the natural ordering of the true DAG  $G$  is unknown, we randomly pick a permutation  $\pi$  for the nodes and apply Algorithm 1 on  $\tilde{X} := XP_\pi$  to estimate  $\Sigma$ . Based on Lemma 1, the  $\hat{\Sigma}$  output from Algorithm 1 is still expected to be a good estimate of  $\Sigma$ , as it is invariant under column-permutation of  $X$ . Then, with the Cholesky factor  $\hat{L}$  of  $\hat{\Theta} (= \hat{\Sigma}^{-1})$ , we de-correlate the rows of  $X$  and treat

$$X^* = \hat{L}X \quad (11)$$

as the new data. Since the row correlations in  $X^*$  vanishes, we can apply any other structure learning method, which assumes independence among observations, on  $X^*$  to learn the underlying DAG. We find that this de-correlation step is able to substantially improve the accuracy of structure learning by well-known state-of-the-art methods, such as the greedy equivalence search (GES) [4] and the PC algorithm [26]. See Section 3 for more details.

---

**Algorithm 1:** Block coordinate descent

---

**Input** :  $X, \Theta^{init}, D^{init}, \Phi^{init}, \tau, T$ **Output** :  $\hat{B}, \hat{\Theta}, \hat{\Omega}$ 

```
while changes in  $\hat{\Theta}, \hat{D}, \hat{\Phi} > \tau$  and  $t < T$  do
  for  $j = 1, \dots, p$  do
     $\hat{\phi}_j^{(t)} \leftarrow$  Lasso regression (8)
     $\hat{\rho}_j^{(t)} \leftarrow$  Quadratic polynomial minimization (9)
  end
   $\hat{\Theta}^{(t)} \leftarrow$  glasso( $\hat{D}^{(t)}, \hat{\Phi}^{(t)}$ ) with support and normalization (10)
  if  $\hat{\Theta}^{(t)}$  decreases the objective function in (10) then
    keep  $\hat{\Theta}^{(t)}$ ;
  else
    update  $\hat{\Theta}^{(t)}$  by line search between  $\hat{\Theta}^{(t)}$  and  $\hat{\Theta}^{(t-1)}$ 
  end
end
 $\hat{\Omega} \leftarrow \hat{D}^{-1}, \hat{B} \leftarrow \hat{\Phi} \cdot \hat{\Omega}^{\frac{1}{2}}$ 
```

---

### 2.3 Some theoretical properties

We first show in Theorem 2 that the likelihood score satisfies the desired score-equivalence property under our proposed model. That is, two DAGs that are Markov equivalent have an identical likelihood score. This property allows us to evaluate estimated DAG structures using common model selection criterion such as AIC and BIC. For example, as we will show in the simulation studies, we can use BIC scores to select the optimal penalty level for the BCD algorithm. Due to the row correlation among data, we cannot directly apply the well-known score-equivalence properties for Markov equivalent DAGs. Write (5) as  $L(B, \Omega, \Theta | X)$  when the DAG is parametrized by  $(B, \Omega)$  and denote by  $(\hat{B}(G), \hat{\Omega}(G), \hat{\Theta}(G))$  the MLE given a DAG  $G$  and the support restriction on  $\Theta$  as in (6).

**Theorem 2.** Suppose  $G_1$  and  $G_2$  are two Markov equivalent DAGs on the same set of  $p$  nodes. If the MLEs  $(\hat{B}(G_m), \hat{\Omega}(G_m), \hat{\Theta}(G_m))$ ,  $m = 1, 2$ , exist for the matrix  $X = (x_{ij})_{n \times p}$ , then

$$L(\hat{B}(G_1), \hat{\Omega}(G_1), \hat{\Theta}(G_1) | X) = L(\hat{B}(G_2), \hat{\Omega}(G_2), \hat{\Theta}(G_2) | X). \quad (12)$$

The next result establishes the convergence of block coordinate descent to a stationary point of the objective function in (6). The stationary point here is defined as a point where all directional derivatives are nonnegative [28].

**Proposition 3.** Let  $\{(\Phi, D, \Theta)^{(t)} : t = 1, 2, \dots\}$  be a sequence generated by block coordinate descent that cycles through  $\Phi, D, \Theta$  to minimize (6) for any  $\lambda_1, \lambda_2 > 0$ . Then for almost all  $X \in \mathbb{R}^{n \times p}$ , every cluster point of  $\{(\Phi, D, \Theta)^{(t)}\}$  is a stationary point of the objective function in (6).

Although Algorithm 1 is not strictly a block coordinate descent algorithm due to the inexact minimization over  $\Theta$  with the line search step, we have not encountered any convergence issue in practice.

See Supplementary Material for the proofs of Theorem 2 and Proposition 3.

## 3 Numerical experiments

If the data we collect from a DAG are indeed correlated via links in a network, we expect the BCD algorithm, which takes these correlations into account, to estimate the DAG structure more accurately than methods that treat the observations as independent. When the natural ordering of the DAG is unknown, the BCD algorithm may still give an accurate estimate of the row correlations that are invariant to node permutation (Lemma 1), which can then be used to de-correlate the observations. We will first test these thoughts on simulated networks for both cases when the nodes are sorted and unsorted. Then, we will provide more results on data generated from real networks.

To apply the BCD algorithm, we need to set the values for  $\lambda_1$  and  $\lambda_2$ . Since the support of  $\Theta$  is known, we simply fixed  $\lambda_2 = 0.01$  in all the results. For each data set, we computed a solution path from the largest  $\lambda_{1 \max}$ , for which we get an empty DAG, to  $\lambda_{1 \min} = \lambda_{1 \max}/100$ . The optimal  $\lambda_1$  was then chosen by minimizing the BIC score over the DAGs on the solution path.

### 3.1 Performance on simulated networks

We generated random DAGs with  $p$  nodes and fixed the total number of edges  $s_0$  in each DAG to  $2p$ . The entries in the weighted adjacency matrix  $B$  of each DAG were drawn uniformly from  $[-1, -0.1] \cup [0.1, 1]$ , and  $\omega_j$ 's were sampled uniformly from  $[0.1, 1]$ . In our simulations, we focused on networks with a clustering structure. We fixed the size of a cluster  $b$  to 20 or 30, and within each cluster, the individuals were correlated according to four covariance structures ( $\Sigma_{ii} = 1, \forall i$ ). 1) Toeplitz:  $\Sigma_{ij} = 0.3^{|i-j|/5}$ . 2) Equi-correlation:  $\Sigma_{ij} = 0.7$ . 3) Star-shaped:  $\Sigma_{ij} = a, \forall i = 1$  or  $j = 1, i \neq j$ ;  $\Sigma_{ij} = a^2$  if  $i \neq j \neq 1$ , where  $a \sim \mathcal{U}([0.3, 0.5])$ . 4) Autoregressive:  $\Sigma_{ij}^{-1} = 0.7^{|i-j|}$  if  $|i-j| \leq \lceil b/4 \rceil$ ;  $\Sigma_{ij}^{-1} = 0$  otherwise. Toeplitz covariance structure implies the observations are correlated as in a Markov chain. Equi-correlation structure is on the opposite of the spectrum, where all observations are conditionally dependent. Star-shaped and AR structures capture intermediate dependence levels. Consequently, the true  $\Theta$  was block-diagonal in our simulations. We evaluated the BCD algorithm and its competitors with two data sizes,  $(n, p) \in \{(200, 100), (100, 300)\}$ . For each  $(n, p)$  and each type of covariances, we simulated 10 random DAGs and then generated one data set following equation (2) for each DAG. Thus, we had 10 results for each of the  $2 \times 4 = 8$  simulation settings. In the end, we averaged the results under each setting for comparison.

Assuming the ordering of the nodes is provided, we compare our BCD algorithm against a similar benchmark BCD algorithm which fixes  $\Theta = I_n$ . In other words, the benchmark algorithm ignores the dependencies among observations when estimating the DAG. Among other estimates, both algorithms return an estimated weighted adjacency matrix  $\hat{B}$  for the optimal  $\lambda_1$  selected by BIC. We then hard-threshold entries in  $\hat{B}$  at a threshold value  $\tau$  to obtain an estimated DAGs. Figure 2 plots the ROC curves of both methods for a sequence of  $\tau$  values under the 8 simulation settings. It is seen that BCD algorithm uniformly outperformed the benchmark in terms of the area under the curve (AUC), with substantial margins for most settings.

To compare the two methods for learning a single DAG, we chose the threshold values so that they predicted roughly the same number of edges  $P$ . Then we calculated the numbers of true positives (TP), false positives (FP) and false negatives (FN), and two overall accuracy metrics Jaccard index ( $TP / (FP + s_0)$ ) and structural Hamming distances (SHD = FP+FN). Note that there were no reserved edges (R) since the ordering was given. Detailed comparisons are summarized in Table 1 in the Supplementary Material, from which we see that the BCD algorithm increased TP while simultaneously decreased FP for every case. The improvement was very significant for the Toeplitz and equi-correlation  $\Sigma$ .

When the natural ordering is unknown, we focus on estimating the row-wise correlation  $\Sigma$ . Given  $\hat{\Sigma}$  we can de-correlate all observations and apply existing structural learning methods on the de-correlated data. In this study, we examine the performance of two well-known structure learning methods before and after de-correlation: GES [4] which is score-based and PC [26] which is constraint-based, implemented in the packages `rcausal` [21] and `pca1g` [16], respectively. Both methods rely on independent data assumption; therefore, we expect the de-correlation step will improve their performances significantly. Different from the previous comparison, GES and PC return an estimated CPDAG (completed acyclic partially directed graph) instead of a DAG. Thus, in the following comparisons, all metrics are calculated with respect to CPDAGs.

As before, we divided the test cases into  $n < p$  and  $n > p$ . The block size for  $\Theta$  was fixed to 30. The estimated Cholesky factor  $\hat{L}$  of  $\hat{\Theta}$ , used for de-correlating  $X$  in (11), was calculated by our BCD algorithm with tuning parameter  $\lambda_1$  selected by BIC. Figure 3 shows the reduction in SHD via de-correlation for both GES and PC on 10 random DAGs generated under each row-covariance structure and each sample size. For almost all types of covariances and  $(n, p)$  settings we considered, the boxplots are way above zero, showing significant improvement of both PC and GES in estimating the CPDAG structures after de-correlation. Detailed results can be found in Table 2 in Supplementary Material.

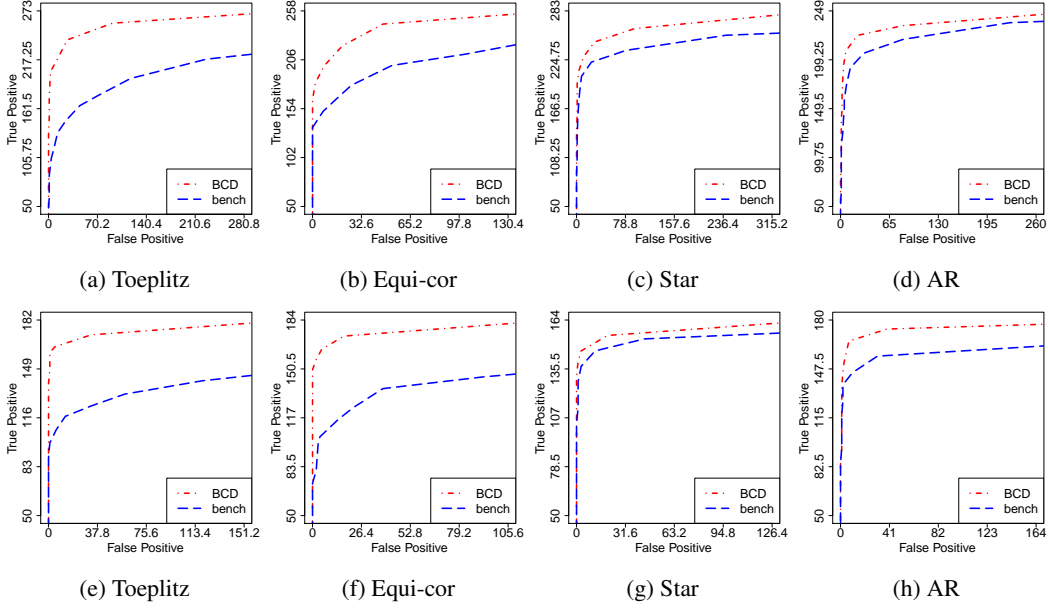


Figure 2: ROC curves of BCD and benchmark BCD on simulated DAGs. Top row:  $n = 100, p = 200$ . Bottom row:  $n = 300, p = 100$ . Block size  $b = 20$ .

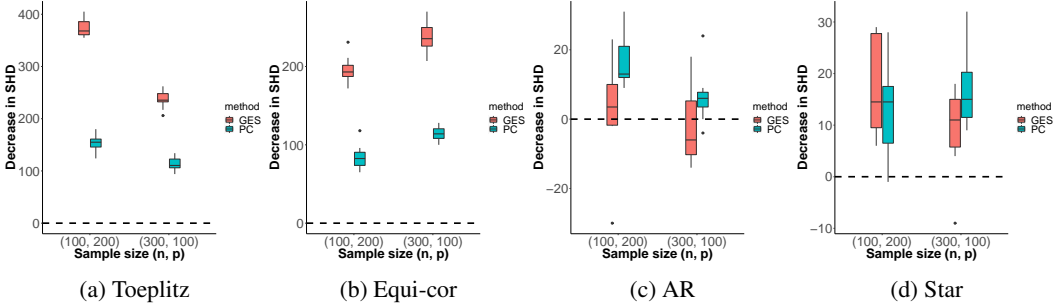


Figure 3: Decrease in SHDs of GES and PC results via de-correlation on simulated DAGs.

### 3.2 Performance on real network structures

Next, we examine the performance of our BCD algorithm on three real DAGs from the bnlearn repository [25]: *andes* [10], *barley* [17], and *hailfinder* [1], and two real undirected networks from *tnet*: *facebook* [19] and *celegans\_n306* [30]. For our simulations, we set the size of DAGs to roughly 200 by replicating some of the above DAGs. 1) *andes*:  $p = 223, s_0 = 338$ . 2) 4 copies of *barley*:  $p = 192, s_0 = 336$ . 3) 4 copies of *hailfinder*:  $p = 224, s_0 = 264$ . On the other hand, we subsampled  $n = 100$  nodes from each of the two undirected networks, *facebook* and *celegans\_n306*, in each simulation. The entries of  $B$  in the DAGs were simulated in the same way as in Section 3.1. The non-zero values in  $\Theta$  for the undirected networks were first generated uniformly from  $[-5, 5]$  and then, a positive constant was added to the diagonal to ensure  $\Theta$  be positive definite; finally,  $\Theta$  was normalized so that  $\text{diag}(\Theta^{-1}) = 1$ . Note that in this experiment,  $\Theta$  was not block-diagonal in general.

Similar as before, for sorted DAGs, we compared the performance between BCD and the benchmark (fixing  $\Theta = I_n$ ) by plotting their ROC curves in Figure 4. Again, for all the combinations of the DAGs and undirected networks, BCD uniformly outperformed the benchmark in terms of AUC, demonstrating the importance in modeling correlations among individuals. We leave more detailed comparisons to Table 3 in Supplementary Material, where we see our BCD method also beat the benchmark in terms of learning DAGs with comparable number of edges.

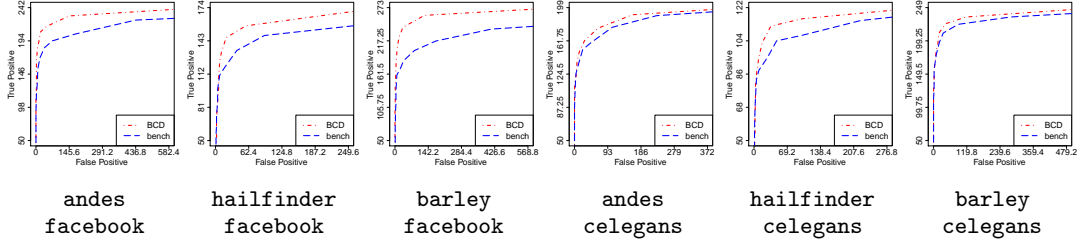


Figure 4: ROC curves of BCD and benchmark BCD on all combinations of real DAGs and undirected networks.

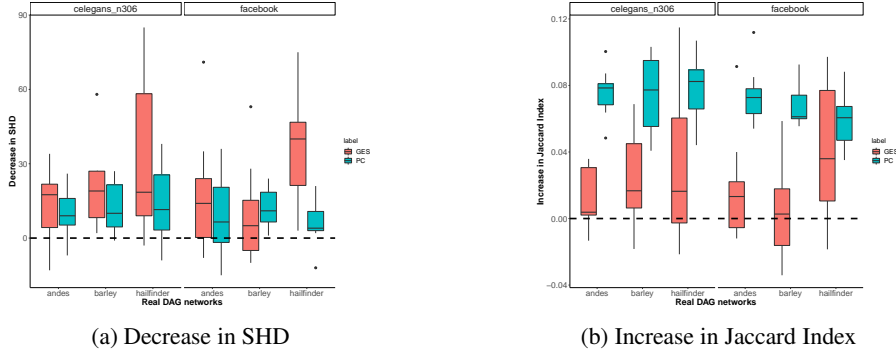


Figure 5: Boxplots of the decrease in SHD and increase in Jaccard index of GES and PC results by de-correlation over data sets from real networks.

For unsorted DAGs, we compared the results of GES and PC applied on original data and de-correlated data, following the same procedure used for simulated DAGs. Figure 5 shows the changes in SHD and Jaccard index. It is clear that for all the real networks we considered, de-correlation with the  $\hat{\Theta}$  estimated by our algorithm decreased the SHDs and increased the Jaccard indices for both methods uniformly. As reported in Table 4 in Supplementary Material, our de-correlation step substantially reduced the FP for GES and increased the TP for PC, leading to clear decrease in SHD and increase in the Jaccard index.

## 4 Summary and future work

We introduced a new DAG model to account for correlations among individuals linked in a network, which is a natural generalization of traditional Gaussian DAGs. We developed the BCD algorithm, based on maximum penalized likelihood, to jointly estimate the row-wise correlation in the data and the structure of the DAG by incorporating this dependence information, given a natural ordering of the nodes. When the ordering is unknown, we showed empirically that our BCD method can accurately estimate the row-wise correlation with a random ordering, thanks to a nice invariant property of the row-wise correlation under our model. Existing methods for structural learning of DAGs, either score-based or constraint-based, assume the availability of i.i.d. data. Therefore, the estimated row correlation by our method can be used to de-correlate network data so that many existing structural learning methods can be applied. From our experiments, this de-correlation approach is able to significantly improve the structure learning accuracy of state-of-the-art methods, such as GES and PC algorithms.

As future work, we will develop error bounds on  $\hat{B}$  and  $\hat{\Theta}$  to rigorously establish the consistency of these estimators. We will also investigate possible improvements of the BCD algorithm for estimating unsorted DAGs, such as incorporating existing order search methods or iterating between de-correlation of data with  $\hat{\Theta}$  and structure learning of DAGs or CPDAGs.



## References

- [1] B. Abramson, J. Brown, W. Edwards, A. Murphy, and R. L. Winkler. Hailfinder: A Bayesian system for forecasting severe weather. *International Journal of Forecasting*, 12(1):57–71, 1996.
- [2] Genevera I Allen and Robert Tibshirani. Transposable regularized covariance models with an application to missing data imputation. *The Annals of Applied Statistics*, 4(2):764, 2010.
- [3] Bryon Aragam and Qing Zhou. Concave penalized estimation of sparse gaussian bayesian networks. *Journal of Machine Learning Research*, 16:2273–2328, 2015.
- [4] David Maxwell Chickering. Optimal structure identification with greedy search. *Journal of Machine Learning Research*, 3:507–554, March 2003.
- [5] Gregory F. Cooper and Edward Herskovits. A bayesian method for the induction of probabilistic networks from data. *Machine Learning*, 9(4):309–347, Oct 1992.
- [6] Pierre Dutilleul. The mle algorithm for the matrix normal distribution. *Journal of Statistical Computation and Simulation*, 64(2):105–123, 1999.
- [7] Gideon E. Schwarz. Estimating the dimension of a model. *The Annals of Statistics*, 6, 03 1978.
- [8] Jerome Friedman, Trevor Hastie, and Robert Tibshirani. Sparse inverse covariance estimation with the graphical lasso. *Biostatistics*, 9(3):432–441, 2008.
- [9] Fei Fu and Qing Zhou. Learning sparse causal gaussian networks with experimental intervention: regularization and coordinate descent. *Journal of the American Statistical Association*, 108(501):288–300, 2013.
- [10] Abigail S. Gertner and Kurt VanLehn. Andes: A coached problem solving environment for physics. In Gilles Gauthier, Claude Frasson, and Kurt VanLehn, editors, *Intelligent Tutoring Systems*, pages 133–142, Berlin, Heidelberg, 2000. Springer Berlin Heidelberg.
- [11] Jiaying Gu, Fei Fu, and Qing Zhou. Penalized estimation of directed acyclic graphs from discrete data. *Statistics and Computing*, 29(1):161–176, 2019.
- [12] José Gámez, Juan Mateo, and Jose Puerta. Learning bayesian networks by hill climbing: Efficient methods based on progressive restriction of the neighborhood. *Data Mining and Knowledge Discovery*, 22:106–148, 05 2011.
- [13] Trevor Hastie, Robert Tibshirani, and Martin Wainwright. *Statistical Learning with Sparsity: The Lasso and Generalizations*. Chapman & Hall/CRC, 2015.
- [14] David Heckerman, Dan Geiger, and David M. Chickering. Learning bayesian networks: The combination of knowledge and statistical data. *Machine Learning*, 20(3):197–243, Sep 1995.
- [15] Dirk Husmeier. Sensitivity and specificity of inferring genetic regulatory interactions from microarray experiments with dynamic bayesian networks. *Bioinformatics*, 19(17):2271–2282, 2003.
- [16] Markus Kalisch, Martin Mächler, Diego Colombo, Marloes H. Maathuis, and Peter Bühlmann. Causal inference using graphical models with the R package pcalg. *Journal of Statistical Software*, 47(11):1–26, 2012.
- [17] Kristian Kristensen and I Rasmussen. A decision support system for mechanical weed control in malting barley. In *Proceedings of the First European Conference on Information Technology in Agriculture*, pages 447–452, 1997.
- [18] Donald Metzler and W Bruce Croft. Combining the language model and inference network approaches to retrieval. *Information processing & management*, 40(5):735–750, 2004.
- [19] Tore Opsahl and Pietro Panzarasa. Clustering in weighted networks. *Social Networks*, 31(2):155 – 163, 2009.
- [20] Judea Pearl. Causal diagrams for empirical research. *Biometrika*, 82(4):669–688, 12 1995.
- [21] Joseph Ramsey, Madelyn Glymour, Ruben Sanchez-Romero, and Clark Glymour. A million variables and more: the fast greedy equivalence search algorithm for learning high-dimensional graphical causal models, with an application to functional magnetic resonance images. *International Journal of Data Science and Analytics*, 3(2):121–129, Mar 2017.

- [22] Teemu Roos. *Minimum Description Length Principle*, pages 823–827. Springer US, Boston, MA, 2017.
- [23] Mauro Scanagatta, Giorgio Corani, Cassio P de Campos, and Marco Zaffalon. Learning treewidth-bounded bayesian networks with thousands of variables. In D. D. Lee, M. Sugiyama, U. V. Luxburg, I. Guyon, and R. Garnett, editors, *Advances in Neural Information Processing Systems 29*, pages 1462–1470. Curran Associates, Inc., 2016.
- [24] Mark Schmidt, Alexandru Niculescu-Mizil, and Kevin Murphy. Learning graphical model structure using l1-regularization paths. In *Proceedings of the 22Nd National Conference on Artificial Intelligence - Volume 2, AAAI’07*, pages 1278–1283. AAAI Press, 2007.
- [25] Marco Scutari. Learning bayesian networks with the bnlearn r package. *Journal of Statistical Software, Articles*, 35(3):1–22, 2010.
- [26] Peter Spirtes, Clark N Glymour, Richard Scheines, David Heckerman, Christopher Meek, Gregory Cooper, and Thomas Richardson. *Causation, prediction, and search*. MIT press, 2000.
- [27] Jin Tian, Changsung Kang, and Judea Pearl. A characterization of interventional distributions in semi-markovian causal models. In *Proceedings of The National Conference on Artificial Intelligence*, volume 21, page 1239. Menlo Park, CA; Cambridge, MA; London; AAAI Press; MIT Press; 1999, 2006.
- [28] P. Tseng. Convergence of a block coordinate descent method for nondifferentiable minimization. *Journal of Optimization Theory and Applications*, 109(3):475–494, Jun 2001.
- [29] Theodoros Tsiligkaridis, Alfred O Hero III, and Shuheng Zhou. On convergence of kronecker graphical lasso algorithms. *IEEE transactions on signal processing*, 61(7):1743–1755, 2013.
- [30] Duncan J Watts and Steven H Strogatz. Collective dynamics of ‘small-world’ networks. *nature*, 393(6684):440, 1998.
- [31] Qiaoling Ye, Arash A. Amini, and Qing Zhou. Optimizing regularized cholesky score for order-based learning of bayesian networks, 2019. arXiv:1904.12360.
- [32] Jiji Zhang. On the completeness of orientation rules for causal discovery in the presence of latent confounders and selection bias. *Artificial Intelligence*, 172(16):1873 – 1896, 2008.
- [33] Shuheng Zhou et al. Gemini: Graph estimation with matrix variate normal instances. *The Annals of Statistics*, 42(2):532–562, 2014.

## Supplementary Material

### Proof of Theorem 2

*Proof.* Let  $L(\tilde{B}(G), \tilde{\Omega}(G), \Theta_0 | X)$  be the maximum likelihood value restricted to the DAG structure  $G$  while fixing  $\Theta = \Theta_0$ . We first show that

$$L(\tilde{B}(G_1), \tilde{\Omega}(G_1), \Theta_0 | X) = L(\tilde{B}(G_2), \tilde{\Omega}(G_2), \Theta_0 | X) \quad (13)$$

for any positive definite  $\Theta_0$ . Let  $L_0$  be the Cholesky factor of  $\Theta_0$ . It is easy to see that we have  $L(B, \Omega, \Theta_0 | X) = L(B, \Omega, I | L_0 X) + p \log \det \Theta_0$ . Consequently, (13) holds, since Gaussian DAG likelihood of i.i.d. data,  $L(B, \Omega, I | L_0 X)$ , is score-equivalent.

Now consider the MLEs  $\hat{B}(G_m), \hat{\Omega}(G_m), \hat{\Theta}(G_m)$  for  $m = 1, 2$ . By definition,

$$\begin{aligned} L(\hat{B}(G_1), \hat{\Omega}(G_1), \hat{\Theta}(G_1)) &= L(\tilde{B}(G_1), \tilde{\Omega}(G_1), \hat{\Theta}(G_1) | X) \\ &= L(\tilde{B}(G_2), \tilde{\Omega}(G_2), \hat{\Theta}(G_1) | X) \\ &\leq L(\hat{B}(G_2), \hat{\Omega}(G_2), \hat{\Theta}(G_2)), \end{aligned}$$

where the second equality is due to (13) and the last inequality follows from the fact that  $\hat{B}(G_2), \hat{\Omega}(G_2), \hat{\Theta}(G_2)$  is the MLE restricted to DAG  $G_2$ . Now using the same argument one can show that

$$L(\hat{B}(G_2), \hat{\Omega}(G_2), \hat{\Theta}(G_2)) \leq L(\hat{B}(G_1), \hat{\Omega}(G_1), \hat{\Theta}(G_1)),$$

and thus the two sides must be identical. This completes the proof.  $\square$

### Proof of Proposition 3

*Proof.* Denote the objective function in (6) as

$$f(\Phi, D, \Theta) = L(\Phi, D, \Theta | X) + \lambda_1 \|\Phi\|_1 + \lambda_2 \|\Theta\|_1.$$

Define the following sets,

$$\begin{aligned} A_1 &= \{\Phi = (\phi_{ij})_{p \times p} \mid \phi_{ij} = 0 \text{ if } j \leq i\}, \\ A_2 &= \{D = \text{diag}\{\rho_1^2, \dots, \rho_p^2\} \mid \rho_j^2 > 0, j \in [p]\}, \\ A_3 &= \{\Theta \mid \Theta \in \mathbb{S}_{++}^n \text{ and } \text{diag}(\Theta^{-1}) = 1\}, \end{aligned}$$

where  $\mathbb{S}_{++}^n$  is the set of  $n \times n$  positive definite matrices. Denote the domain of  $f(\Phi, D, \Theta)$  by

$$\text{dom} f = \{(\Phi, D, \Theta) \mid \Phi \in A_1, D \in A_2, \Theta \in A_3\}.$$

Then,  $f$  can be represented as the sum of a differentiable function,  $L(\Phi, D, \Theta | X)$ , and a continuous function,  $\lambda_1 \|\Phi\|_1 + \lambda_2 \|\Theta\|_1$  on  $\text{dom} f$ . Since  $\text{dom} f$  is open, by Lemma 3.1 in [28],  $f$  is regular at each  $(\Phi, D, \Theta) \in \text{dom} f$ . For any  $\Theta \in A_3$ , let  $L$  be its Cholesky factor such that  $\Theta = L^\top L$ . For almost all  $X$ , the columns of  $LX$  are in *general position* and thus the lasso solution for  $X_j$  on  $X_i, i < j$  is unique [13, p.19]. Consequently,  $f$  has at most one minimizer in  $D$  and  $\Phi$ , separately. Then, Theorem 4.1 (c) in [28] implies that the block coordinate descent that cycles through  $\Phi, D, \Theta$  converges to a stationary point of  $f$ .  $\square$

Supplementary Tables

Table 1: Results for ordered DAGs on simulated data. Block size  $b = 20$ .

$(n, p)$	$\Theta$ -type	Algorithm	P	TP	FP	FDR	JI	SHD
(100, 200)	Toeplitz	BCD	207.9	205.6	2.3	0.01	0.51	196.7
		bench	206.6	168.3	38.3	0.18	0.38	270.0
	Equi.cor	BCD	194.2	192.4	1.8	0.01	0.48	209.4
		bench	194.4	158.9	35.5	0.17	0.37	276.6
	AR	BCD	196.5	193.2	3.3	0.02	0.48	210.1
		bench	196.1	187.0	9.1	0.05	0.46	222.1
	Star	BCD	219.2	217.2	2.0	0.01	0.54	184.8
		bench	215.3	207.9	7.4	0.03	0.51	199.5
(300, 100)	Toeplitz	BCD	146.1	146.0	0.1	0.00	0.73	54.1
		bench	144.3	121.8	22.5	0.15	0.55	100.7
	Equi.cor	BCD	136.1	136.1	0.0	0.00	0.68	63.9
		bench	138.7	122.4	16.3	0.12	0.57	93.9
	AR	BCD	131.0	130.6	0.4	0.01	0.65	69.8
		bench	131.8	129.8	2.0	0.01	0.64	72.2
	Star	BCD	127.4	126.6	0.8	0.01	0.63	74.2
		bench	126.5	124.7	1.8	0.01	0.62	77.1

The average number of predicted (P), true positive (TP), false positive (FP) edges, the average False Discovery Rate (FDR), Jaccard index (JI), and Structural Hamming Distance (SHD) for DAGs learned by the two BCD algorithms.

Table 2: Results for unordered DAGs on simulated data. Block size  $b = 30$ .

$(n, p)$	$\Theta$ -type	Algorithm	P	TP	FP	R	JI	SHD
(100, 200)	Toeplitz	GES	444.1	114.7	329.4	54.9	0.16	669.6
		GES-L	166.9	161.1	5.8	51.3	0.40	296.0
		PC	206.3	79.4	126.9	59.1	0.15	506.6
		PC-L	185.7	171.4	14.3	110.5	0.41	353.4
	Equi.cor	GES	315.3	129.6	185.7	58.4	0.22	514.5
		GES-L	144.6	140.8	3.8	56.6	0.35	319.6
		PC	155.7	95.4	60.3	67.0	0.21	431.9
		PC-L	172.9	162.9	10.0	100.6	0.40	347.7
	AR	GES	176.2	162.5	13.7	52.9	0.39	304.1
		GES-L	160.4	154.4	6.0	49.8	0.38	301.4
		PC	147.3	137.3	10.0	92.4	0.33	365.1
		PC-L	179.8	169.2	10.6	107.2	0.41	348.6
Star	GES	181.4	161.1	20.3	53.7	0.38	312.9	
	GES-L	163.9	159.3	4.6	50.0	0.39	295.3	
	PC	142.2	132.5	9.7	86.7	0.32	363.9	
	PC-L	183.2	171.1	12.1	110.0	0.42	351.0	
(300, 100)	Toeplitz	GES	307.2	104.6	202.6	38.6	0.26	336.6
		GES-L	126.0	122.0	4.0	18.2	0.60	100.2
		PC	163.2	78.6	84.6	58.2	0.28	264.2
		PC-L	133.3	128.9	4.4	75.7	0.63	151.2
	Equi.cor	GES	314.4	101.0	213.4	39.0	0.24	351.4
		GES-L	112.5	109.4	3.1	20.7	0.54	114.4
		PC	155.7	71.6	84.1	52.7	0.25	265.2
		PC-L	123.8	121.1	2.7	69.4	0.60	151.0
	AR	GES	129.1	122.0	7.1	18.6	0.59	103.7
		GES-L	120.3	115.8	4.5	17.3	0.57	106.0
		PC	115.1	112.1	3.0	67.2	0.55	158.1
		PC-L	128.7	124.5	4.2	72.0	0.61	151.7
Star	GES	133.4	123.3	10.1	21.3	0.59	108.1	
	GES-L	125.9	122.3	3.6	17.4	0.60	98.7	
	PC	117.0	108.6	8.4	64.2	0.52	164.4	
	PC-L	132.1	128.1	4.0	71.7	0.63	146.6	

The average number of predicted (P), true positive (TP), false positive (FP), reversed (R) edges, the average Jaccard index (JI), and Structural Hamming Distance (SHD) for CPDAGs learned by the GES and PC algorithms before and after de-correlating the data with the estimated Cholesky factor  $\hat{L}$  by the BCD. GES-L and PC-L represent GES and PC methods, respectively, on the de-correlated data.

Table 3: Results for ordered DAGs on real networks.

Undirected network	DAG	Algorithm	P	TP	FP	FDR	JI	SHD
facebook	andes	BCD	200.0	187.4	12.6	0.06	0.53	163.2
		bench	197.7	178.2	19.5	0.09	0.50	179.3
	hailfinder	BCD	150.2	135.4	14.8	0.10	0.49	143.4
		bench	147.2	128.0	19.2	0.13	0.45	155.2
	barley	BCD	273.2	241.9	31.3	0.11	0.54	209.4
		bench	270.5	232.1	38.4	0.14	0.51	226.3
celegans_n306	andes	BCD	132.9	125.7	7.2	0.05	0.36	219.5
		bench	133.0	124.6	8.4	0.06	0.36	221.8
	hailfinder	BCD	135.3	107.9	27.4	0.20	0.37	183.5
		bench	139.9	97.6	42.3	0.29	0.32	208.7
	barley	BCD	196.2	146.7	49.5	0.25	0.38	238.8
		bench	189.7	141.4	48.3	0.24	0.37	242.9

Table 4: Results for unordered DAGs on real networks.

Undirected network	DAG	Algorithm	P	TP	FP	R	JI	SHD
facebook	andes	GES	73.3	59.0	14.3	18.2	0.16	108.7
		GES-L	61.0	58.5	2.5	17.9	0.17	97.1
		PC	57.9	51.0	6.9	33.4	0.14	124.5
		PC-L	72.2	62.2	10.0	37.3	0.17	120.3
	hailfinder	GES	167.7	131.6	36.1	62.4	0.44	230.9
		GES-L	141.2	131.8	9.4	51.2	0.48	192.8
		PC	119.1	98.6	20.5	52.7	0.35	238.6
		PC-L	145.1	118.3	26.8	60.1	0.41	232.6
	barley	GES	180.8	151.2	29.6	60.1	0.41	274.5
		GES-L	165.5	148.0	17.5	59.7	0.42	265.2
		PC	136.0	121.4	14.6	78.7	0.35	307.9
		PC-L	165.0	146.6	18.4	88.2	0.41	296.0
celegans_n306	andes	GES	180.4	149.0	31.4	40.4	0.40	260.8
		GES-L	149.7	143.4	6.3	46.3	0.42	247.2
		PC	143.6	123.0	20.6	75.6	0.34	311.2
		PC-L	176.4	151.9	24.5	90.5	0.42	301.1
	hailfinder	GES	165.4	133.3	32.1	64.5	0.45	227.3
		GES-L	138.1	130.7	7.4	54.2	0.48	194.9
		PC	121.8	98.1	23.7	52.8	0.34	242.4
		PC-L	149.5	122.4	27.1	59.5	0.42	228.2
	barley	GES	182.0	147.3	34.7	63.3	0.40	286.7
		GES-L	164.5	148.3	16.2	62.4	0.42	266.3
		PC	139.4	121.7	17.7	74.5	0.34	306.5
		PC-L	164.7	147.9	16.8	89.2	0.42	294.1